43rd AIAA Fluid Dynamics Conference
June 24-27, 2013, San Diego, CA
AIAA 2013-2608

Developing Mechanism-Based Methods for Estimating Hypersonic Boundary-Layer Transition in Flight: The Role of Quiet Tunnels

Steven P. Schneider*
School of Aeronautics and Astronautics
Purdue University
West Lafayette, IN 47907-1282

Abstract

For more than half a century, researchers have been aware that freestream fluctuations have an important effect on laminar-turbulent transition. A century of effort has also been devoted to the development of theory and experiment for the instability mechanisms that lead to transition, in order to develop more reliable prediction methods. Both of these long efforts are now beginning to bear fruit in the subarea of hypersonic transition. At hypersonic speeds, it was necessary to develop *quiet tunnels* with laminar nozzle-wall boundary layers in order to achieve low fluctuation levels that are comparable to flight; three such tunnels are now in operation, worldwide. Hypersonic instability mechanisms are also more complex than at low speeds, and the computer resources and computational tools necessary to compute them are only now becoming fairly widely available, along with the instrumentation necessary to measure these mechanisms in a reasonably affordable way. The present review begins to show how these two steps are aiding in the development of physics-based methods for estimating transition in flight.

Introduction

General

Laminar-turbulent transition at hypersonic speeds causes large changes in heat transfer, skin friction and boundary-layer separation. Thus, it affects aerodynamic lift and drag, aerodynamic stability and control, the design of the thermal protection system, and maintainability. It also affects the aerooptics above seeker windows. Transition is the readily-observed result of a subtle and complex laminar-instability process. Although the vast low-speed literature gives much insight into the phenomena, hypervelocity flow involves additional instabilities, disturbance sources, and parametric influences that are not present at low speed. Disturbances originate on the body or in the freestream [1]. The receptivity mechanisms by which the disturbances enter a boundary layer are influenced by ablation, roughness, waviness, bluntness, curvature, Mach number, and so on [2]. The various disturbances are amplified by one or several instabilities, which may or may not interact.

The first-mode instability is similar to low-speed Tollmien-Schlichting waves, although it is most amplified when the wavefronts are oblique to the stream direction [3]. It is damped by wall cooling. The second-mode instability is similar to a trapped acoustic wave, and is most amplified when the wavefronts are normal to the stream direction. It grows more rapidly on cold walls and occurs at higher Mach numbers [3, 4]. The cross-flow instability occurs in three-dimensional boundary layers, and has both traveling and stationary forms [5, 6, 7]. The Görtler instability is important for boundary layers on concave walls, and perhaps in some regions of concave streamline curvature [8, 9]. Attachment lines [10], entropy layers [11], roughness [12, 13, 14, 15], and ablation [16] may generate additional instabilities. Transient growth can also lead to large amplification ratios [17]. The first appearance of turbulence is associated with the breakdown of the instability waves, which is determined by various nonlinear mechanisms [18].

These instabilities are in turn affected by all the factors determining the mean boundary layer flow, including Mach number, transverse and streamwise curvature, pressure gradient, chemistry, ablation, and enthalpy [17]. Local spots of turbulence grow downstream through an intermittently-turbulent region whose length is dependent on the local flow

*Professor. Associate Fellow, AIAA.

conditions and on the rate at which spots are generated [19]. Aeroheating in the transitional region often exceeds that which is computed in a fully-turbulent analysis.

In view of the dozens of factors influencing transition, classical attempts to correlate the general transition 'point' with one or two parameters such as Reynolds number and Mach number can be reasonably accurate and reliable only for cases that are similar to those previously tested. Even for relatively simple geometries, Ref. [20] shows the large scatter that is observed in those rare instances when a correlation is attempted using a moderately wide-ranging dataset. Transition-estimation methods that are reliable for a broad range of conditions will need to be based on an understanding of the physical mechanisms involved [21]. Although these are in regular use at lower speeds [22], they are only beginning to become available at hypersonic speeds.

The simplest and best developed of the mechanism-based methods are the e^N methods, which attempt to correlate transition with the integrated growth of the linear instability waves [23]. These methods neglect freestream noise variations, receptivity, and all nonlinear effects, such as wave interactions, nonlinear breakdown effects, and so on. However, they have shown promising agreement with experiment for a variety of conditions where the environmental noise is generally low [24, 25]. Furthermore, there is a long history of extending and calibrating these methods using semi-empirical corrections, with fairly good success (see, for example, Ref. [26]). Although wave interaction effects and 3D effects can sometimes be handled with these kinds of correlations, e^N methods are only an intermediate step along the way to reliable mechanism-based methods. Recent experiments have shown there are substantial limitations to the traditional $N \simeq 10$ approach, even under hypersonic wind-tunnel conditions [27]. Improvements in techniques for estimating the location and extent of transition will depend on improvements in our understanding of the physical mechanisms involved.

Direct simulations of transition [28, 29, 30] and the Parabolized Stability Equations [31] provide advanced theoretical-numerical tools that are capable of simulating very complex physical processes. However, the capabilities of these tools seem far in advance of our understanding of the actual physics of these flows. Many assumptions are still needed to compute realistic flows. It is expensive and difficult to measure the flow details that are necessary to develop and validate the assumptions needed, and few such measurements have been performed. Some of the desirable measurements may not be feasible at all.

For example, very little is known about the freestream disturbance fields that develop into the instability waves. To date, most direct simulations are carried out using arbitrarily-assumed incoming-disturbance fields with very simple forms. This is partly because real-world incoming-disturbance fields are difficult or impossible to measure completely. A full characterization of a wind-tunnel freestream requires measurements of the unsteady vector fields for the vorticity and acoustic waves, of the unsteady scalar field for the entropy spottiness, of the full particulate content, and of all unsteadiness in the freestream chemistry. The measurements should include not only the mean and the spatial variations in the mean, but the spectra of the fluctuations, their spatial variations, and perhaps even two-point correlations of these spectra. These measurements should have substantial signal-to-noise ratio out beyond the second-mode instability frequencies, which may exceed 1 MHz, and where the amplitude of the freestream disturbances is very small [32, 33]. A full set of measurements of these fields is thus far more challenging than at low speeds, and the cost is far higher than at low speeds, due to the energy necessary to generate these flows. Although it is critical to measure as much as possible of this complex disturbance field, feasible measurements within the foreseeable future will be limited to some small fraction of all the desirable quantities. Measurements of the disturbance field in flight will be even more challenging.

Much progress can nevertheless be made by combining advanced computational studies with feasible measurements of the disturbance fields, instability processes and transitional properties. The necessary computational assumptions must be based on the available experimental data and on sensitivity analyses. It will probably be necessary to *calibrate* the disturbance-field inputs by comparing the computational results to the measurements that are feasible. For example, in the future, it appears that direct simulations will need to use computed and calibrated incoming-disturbance fields if they are to be compared with realistic experiments or flight tests [34].

Even with all the computational advances, numerical work is only beginning to include complex effects such as roughness, waviness, and internal shocks. Three- dimensional mean flows and their instabilities are only beginning to be treated correctly

from first principles [35, 36]. The simulation of ablation and chemistry effects is only beginning [37]. When the numerics are based on the correct physical mechanisms, however, direct numerical simulations can provide much more detail regarding the transition process [38, 39]. Efficient and effective progress in understanding hypersonic instability and transition will require the use of all available approaches, developed in a coordinated way.

Thus, experimental work that describes not only the location of transition but also the mechanisms involved is needed in order to improve these modern theories. The key mechanisms need to be identified, in part through experimental work, and the key numerical assumptions and results need to be validated experimentally. Unfortunately, most of the ground-test data are ambiguous, due to operation in high-noise conventional wind tunnels and shock tunnels, with disturbance levels much higher than in flight [40, 41]. The boundary layer on the wind-tunnel nozzle wall is usually turbulent, and this radiates high levels of noise onto the model. The mechanisms of transition operational in small-disturbance environments can be changed or bypassed altogether in such high-noise environments [42, 32]. Just as at low speed, it is best to conduct ground tests at noise levels comparable to flight, in order to provide reliable and unambiguous measurements of transition mechanisms and trends. However, these quiet noise levels require laminar nozzle-wall boundary layers, and are presently available only in three wind tunnels at Mach 6 and moderate Reynolds numbers, in cold flow [41, 43, 44].

Thus, no single wind tunnel is able to simulate the enthalpy, Mach number, Reynolds number, surface temperature, roughness, scale, freestream perturbations, and surface properties of ablating hypervelocity flight. As for other hypersonic phenomena, simulation of transition therefore involves the art of combining partial experimental simulations using approximate theories and approximate numerical simulations [45]. Flight tests are free from facility noise issues and must constitute the final basis for evaluating transition-estimation techniques. However, they have their own limitations and are very expensive. Accurate and reliable prediction of hypersonic transition for new vehicles will remain a challenge for many years. The ability to lead in these kinds of critical engineering-science areas will contribute to determining who will lead the world in defense technologies.

Mechanisms Likely to be Important for Various Vehicle Classes

Tractable approaches to the complex physics of hypersonic transition will therefore require a focus on the mechanisms that seem most relevant to various types of vehicles. It must be possible to compute the critical aspects of the mechanisms in flight and also for the conditions in preparatory ground tests. It will also be necessary to verify the presence of these mechanisms via measurements during ground tests. It will be necessary to use the computational simulations to compare results from ground tests in different facilities with different kinds of limitations relative to the flight environment. Some ground tests may be able to match Reynolds number and Mach number but only under cold flow with conventional noise levels, some may match enthalpy and scale but only for cold model temperatures and conventional noise levels, some may have quiet noise levels but low Mach and Reynolds numbers. Thus, the computational mechanism-based simulations must account for tunnel noise, enthalpy, Mach and Reynolds number effects. Feasible simulations will need to be calibrated using the ground-test data and previous flight data; thus, they need capture only the critical trends, and not every detail of the complex physical processes.

Timely progress on such a complex problem will require collaboration, even for a carefully restricted subset of the full parameter space. Defense missions will generally involve slender vehicles with lift. If the nose radius is sufficiently small, the second-mode instability may dominate, so it is probably the most important mechanism to focus on. Lifting vehicles will generate three-dimensional flow, and thus the crossflow instability, which might cause transition at lower Reynolds numbers. It may be possible to design the vehicles to minimize crossflow, but some approximate method for estimating the effect of the crossflow instability will still be necessary in order to design away from it. The crossflow instability comes in traveling and stationary forms, which have different sensitivities to tunnel noise and surface roughness. Two different kinds of instrumentation will be needed to measure these two forms of the crossflow instability. For lower freestream Mach numbers, higher nose radii, and larger angles of attack, the first-mode instability may become important, and it will be necessary to determine via computations and measurements whether it is observed under various conditions, and whether it serves an important role in the overall transition process.

Linear and nonlinear growth for these three in-

stabilities can already be computed, at least for perfect-gas conditions, and the second-mode instability has now been measured in numerous perfect-gas tunnels. Codes to compute the instabilities of high-enthalpy three-dimensional flows are in development, although not yet available [46]. Preliminary measurements of the second-mode instability in shock tunnels are becoming available under perfect gas conditions, but the capability is not yet well developed, and is only beginning to be extended to measure the second mode in these same facilities under high-enthalpy conditions [47, 48, 49]. Methods of measuring the traveling and stationary crossflow instability are only beginning to become available [50]. Progress is being reported in all these areas, with several papers being presented at the present conference. The remainder of the present paper will discuss some of the overall issues in these various areas, with emphasis on the contribution from quiet-tunnel measurements.

The author has worked almost exclusively on transition since 1985, and on high-speed transition since 1990, but even an 8000-paper library and database is far from complete; the author still has much to learn about the vast literature for high-speed transition. Thus, the author would appreciate hearing of errors and omissions.

The reader may note that the present paper focuses primarily on the second-mode mechanism. In part, this is because more is known about the second mode; however, in large part this is simply because there wasn't enough time to write a more detailed review of recent progress regarding the other mechanisms.

Mechanism-Based Methods for Second-Mode Transition

Overall Concepts

During the last several years, a number of researchers from Japan, the United States, Germany, Russia and Belgium have been measuring second-mode instabilities and tunnel noise using fast pressure sensors and also fast heat-transfer sensors. Numerous publications have appeared, and a brief summary of some of this work appears in Ref. [51]. If the cold-tunnel work can determine the physics that explains Pate's correlation [52], this same physics could then be used to predict transition induced by second-mode waves on other geometries [53]. Since it is much easier to measure and compute in cold flow, progress is much more rapid. Approaches that are successful in cold flow can then be extended to high-enthalpy flow, as methods are developed to measure second-mode waves in the necessary short-duration shock or expansion tunnels [49].

The second-mode instability on slender cones with small nose radii near zero angle of attack appears to be one of the simplest yet most important cases where the work of various groups is being compared and combined. To simplify comparisons, most researchers are using a 7-deg. half-angle cone and the smallest feasible nose radius (which may not be 'sharp' in the high-enthalpy tunnels). Surface pressure sensors can be readily used to measure the instability waves in most tunnels. The performance of different kinds of sensors can be compared and calibrated, under various conditions. Computations can then extrapolate the measured waves to the onset of instability to infer an initial amplitude. Freestream pitot-pressure measurements can provide an initial characterization of fluctuations, and these can be compared to surface pressure measurements underneath the laminar boundary layer. Freestream stagnation-heating measurements can also be carried out on small probes in most tunnels, to help determine temperature spottiness [54].

If these fluctuation measurements can be extended or extrapolated to the second-mode frequencies [55], with sufficient signal-to-noise ratio, an effective receptivity coefficient can be computed. Does receptivity happen primarily near the leading edge, even under conventional-noise conditions? Since the freestream fluctuations in cold tunnels are probably dominated by the noise radiated from the turbulent boundary layers on the nozzle walls, much is known about them, and much could be determined using direct numerical simulations of the radiated acoustic noise for sample configurations, combined with classical theory for boundary-layer radiated noise, measurements of the nozzle- wall boundary-layer properties, and the measured fluctuations. Initial computations of the noise were recently reported by Duan and Choudhari [34]. How do the measured pitot fluctuations compare to the predictions from Pate's correlation? Can the changes in the initial wave amplitude explain Pate's correlation, or is it necessary to also account for the effect of noise on the breakdown amplitude? What is the effect of the freestream particles that are inevitably present [56, 57]?

The amplification of the waves can then be compared to the computations. When the waves amplify linearly, tunnel noise should not affect the results,

but any nonlinear receptivity processes may be affected by tunnel noise. At what point does the wave amplification become nonlinear? At what conditions do the waves begin to break down to turbulence? Direct numerical simulations are beginning to become available, but these must make many assumptions [58, 59]. Certainly one would expect tunnel noise to affect the nonlinear breakdown as well as the initial amplitude, but can the effect of tunnel noise be sorted out? What correlates with the breakdown conditions for the waves? What affects these breakdown conditions? Measurements in two different Mach-6 tunnels under similar conventional noise yielded similar wave amplitudes at breakdown [60], suggesting that the breakdown is not that dependent on the small details of the disturbance environment.

However, it doesn't seem that this will hold true in general, for Refs. [61, 62] show that the breakdown amplitude increased with Mach number, from 5% at Mach 5 to 12% at Mach 6 and 24% at Mach 8. Whether the increase with Mach number is associated with changes in tunnel noise is not yet clear. To help determine the effect of tunnel noise on the breakdown amplitudes, quiet tunnel measurements will be needed. Since existing quiet tunnels cannot obtain natural transition under fully quiet conditions for a sharp 7-deg. half-angle cone at zero angle of attack, it will be necessary to use special geometries designed to achieve the largest possible second-mode waves, or to use controlled perturbations, or both. A flared cone was designed using the Univ. Minnesota STABL code to achieve very high N factors under fully quiet flow in the Purdue tunnel, and natural transition was apparently achieved under fully quiet flow in the latest iteration [27], so the passive approach seems promising so far. Theoretical and computational advances are greatly needed to complement this kind of experimental approach, but the three research methods must be closely coordinated to achieve effective results, and this is challenging to achieve in practice.

Earlier Measurements of Wave Amplitudes

For many years, it has been possible to compute the linear growth of second-mode waves, and compare the results to experiments under perfect-gas conditions. Most of these experiments have been carried out on slender cones near zero angle of attack (see, for example, Ref. [63]). Reasonably good agreement has been obtained, once the wave amplitude rises above the background noise, and before the waves become large enough to be nonlinear. However, under conventional noise conditions, this range of amplitudes is often fairly small. For example, in Ref. [63] it is about e^2 or less, for both the Stetson and ITAM experiments.

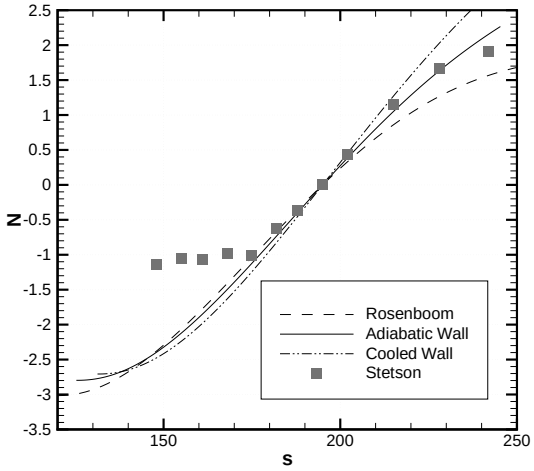

Figure 1: N-factor comparison for Stetson experiment. From Ref. [63, Fig. 11]

Lyttle's comparison to the Stetson experiments is shown in Fig. 11 of Ref. [63], reproduced here as Fig. 1. Here, the arbitrary offset in the vertical scale for the N factors is set so the experiment and computation match up at $N = 0$, at an arc-length location that is 195 nose radii from the stagnation point. Unlike in typical analyses, $N = 0$ is *not* at the onset of the computed amplification. However, the paper notes that the waves grew by about $e^{1.7}$ before rising above the background noise, at about $N = -1$ in Fig. 1. This analysis is for a frequency of about 130kHz. Transition did not occur on Stetson's model for these conditions, so the wave amplitude at transition onset is not available.

With a little more effort, the initial amplitude of the second-mode waves can be inferred from these computations. The Stetson measurements were made on a 7-deg. half-angle cone with a 3.81-mm nose radius at a stagnation pressure of 4.00 MPa and a stagnation temperature of 750 K, as described in more detail in Ref. [64, pp. 13-19]. At an arclength of 195 nose radii or 29.25 inches, this location is very near to $s = 29.231$, where quantitative amplitude data from Stetson's Run 59 is available in Figs. 21 and 22 of Ref. [64]. Since the massflow fluctuations are much larger than the total temperature fluctuations, the former will be the focus here. The Stetson massflow spectra are here replotted as

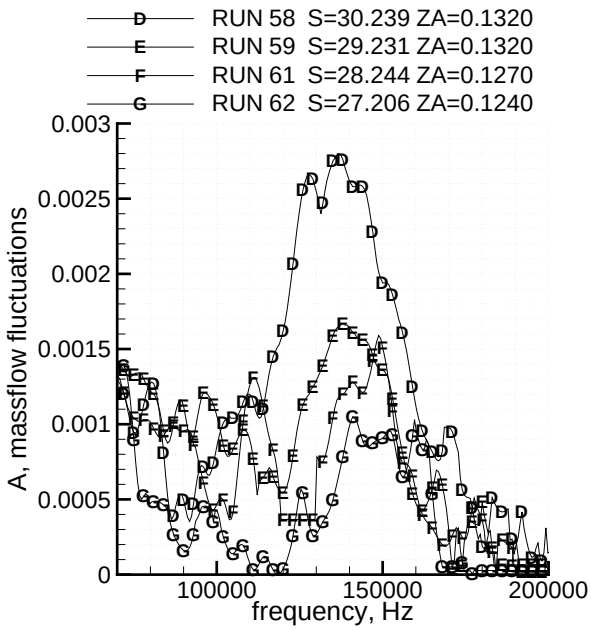

Figure 2: Massflux spectra for Stetson blunt cone. Detail near $s = 29.23$ inches. From Ref. [64, Fig. 21]

Fig. 2, modified so as to show the appropriate detail. Although the normalizations are a little confusing and uncertain, it appears they are given in terms of the amplitude ratio for each spectral interval of 600 Hz. The massflux amplitude of the 130kHz wave is then roughly 0.0013, or 0.13% of the mean massflux. Since the computations show that the waves have grown by $e^{1.7}$ at this point, we can infer an equivalent initial amplitude of about 0.02%. Of course, the instability may be receptive to the high levels of tunnel noise over a large region on the cone, even downstream of the neutral point for this wave; nevertheless it seems useful to infer this initial equivalent amplitude, as a first approximation.

Preliminary comparisons to the freestream noise in this tunnel could almost be made, using the measurements reported in Ref. [65] (see also Ref. [66]). Fig. 6b in Ref. [65] confirms that the freestream massflow fluctuations are an order of magnitude larger than the freestream total-temperature fluctuations. Figs. 7 and 8 in Ref. [65] report normalized power spectra for these fluctuations. However, the signal above 100kHz is a very small fraction of the overall RMS fluctuations of 1-2%, and the signal disappears into the noise near 200kHz at a unit Reynolds number of about 3×10^6/ft. In principal, it should be possible to determine the signal amplitude at 130kHz, and compare it to the 0.02% inferred above, but this would require knowledge of the normalization for Fig. 7 in Ref. [65], or integration of this spectrum so the normalization can be inferred from Fig. 6b. The original data would be needed to make progress in an effective manner; unfortunately, these have apparently been lost. New and improved measurements are therefore needed.

The comparisons to the ITAM experiments are shown in Fig. 18 of Ref. [63], reproduced here as Fig. 3. Here, the waves grew by about $e^{1.3}$ before rising above the background noise, at about $N = -0.1$ in Fig. 3. Here, $N = 0$ at a location that is 300 nose radii in arclength from the stagnation point, or about 0.225 m. The experiment measured a 7-deg. half-angle cone in a Mach-6 blowdown tunnel at a stagnation pressure of 1.0 MPa and a stagnation temperature of 380-395 K. Controlled perturbations were used to enhance the signal-to-noise ratio for the ITAM data shown here [67], so it is not meaningful to infer the initial amplitude at the onset of instability and compare this to the Stetson results.

Under conventional noise, the waves must become fairly large, in order to rise above the background disturbance level that is created by the tunnel-wall radiated noise within the boundary layer. Once the waves become this large, they cannot grow too much larger without becoming nonlinear. However, the waves also begin with a larger amplitude, since they are initialized from a much higher level of freestream fluctuations. Are the onset and development of nonlinearity affected by tunnel noise? If so, how? Quantitive measurements of wave amplitude are needed to help answer this question, and these have always been very challenging, at these high frequencies and small amplitudes. In addition, quiet tunnel measurements are also needed.

Measurements of Wave Amplitudes in the Langley Mach-6 Quiet Tunnel

Part of the answer was obtained during the initial hypersonic quiet-tunnel measurements at NASA Langley during the 1990's [68]. Initially, only transition was measured in the Langley quiet tunnels, to determine the effect of tunnel noise on transition location [41]. However, during the 1990's, three instability-wave projects were carried out before the Mach-6 quiet tunnel was decommissioned. There were no measurements of absolute wave amplitudes due to difficulties with electronic noise and high-frequency hot-wire anemometry. The calibrations

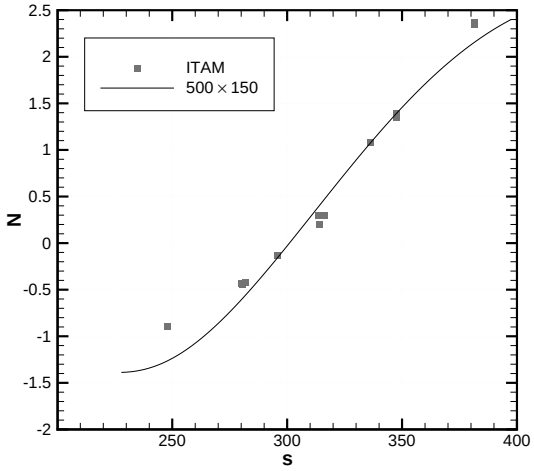

Figure 3: N-factor comparison for ITAM experiment. From Ref. [63, Fig. 18]

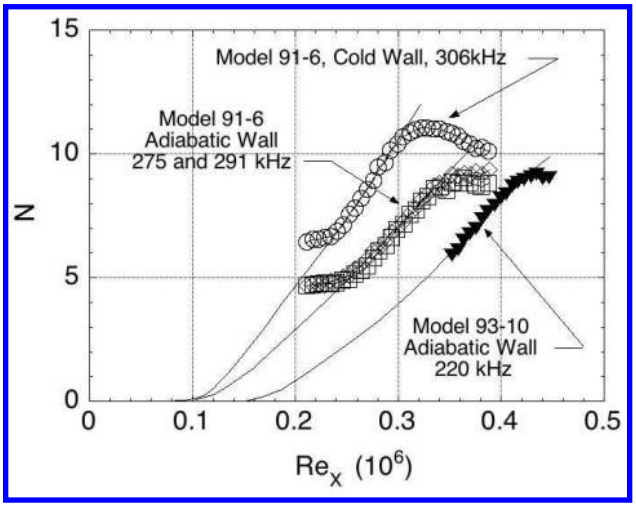

Figure 4: N-factor comparison for NASA Langley experiments. From Ref. [68, Fig. 11]

that were feasible limited the measurements to relative wave amplitudes, not absolute amplitudes. Note that to measure instability waves, it is necessary for them to grow large enough to rise above both the fluid-dynamic background noise *and* the electronic background noise. The latter was a particularly difficult issue for the Mach-6 quiet nozzle as it was installed at the time.

However, Fig. 11 in Ref. [68], reproduced here as Fig. 4, reports N factors (the natural logarithm of the relative wave amplitudes) for two different flared-cone models at two different wall temperature conditions, for a total of three datasets. For the 91-6 model with a cold wall, the 306-kHz second-mode waves rose above the background noise at about $N = 7$ and grew to about $N = 11$ before saturating, apparently at transition onset. For the 91-6 model with an adiabatic wall, the 275 and 291 kHz waves rose above the background noise at about $N = 5$ and grew to about $N = 9$ before transition onset. The 93-10 model with the adiabatic wall yielded 220kHz second-mode waves that were measured from about $N = 6$ to breakdown at $N = 9$ or so. In all cases, transition onset occurred near the end of the quiet region, so it seems possible or likely that transition was affected by noise radiated onto the model from the transitional boundary layer on the nozzle wall [41]. However, this issue remains to be clarified.

In the quiet tunnel, therefore, the waves had to grow much more before their amplitude rose above the background noise – they had to grow by $N \simeq 5 - 7$, rather than by $N \simeq 1 - 2$, as in the two conventional tunnels. There is a large difference of roughly e^{4-5}. This can be expected, since the initial wave amplitudes are much smaller in the quiet tunnels, due to much smaller freestream disturbance levels. Estorf et al. measured second-mode wave amplitudes that were about 450 times smaller under quiet flow than under conventional noise levels, for a 7-deg. half-angle cone in the Purdue tunnel at Mach 6 [60]. Although a factor of 450 or about e^6 is larger than the factor of e^{4-5} described above, it may be that the Purdue tunnel is somewhat quieter than the Langley tunnel was, since Steen measured freestream pitot-pressure fluctuations as low as 0.01% [69]. Further measurements are needed to sort out the effects of electronic noise, freestream fluctuations, and wave amplitudes.

Note also that in the Langley quiet tunnel, the waves grew by factors of about e^4, e^4, and e^3 between the points where they rose out of the noise, and where they became nonlinear. These measurable linear regions are larger than the e^2 regions in the conventional-noise comparisons, but they are still small compared to the nominal e^{10} growth that is expected prior to transition. The Langley data shown in Fig. 4 seems to support the traditional N-factors that are expected at transition (about 9-10), since those are the maximum values achieved prior to the onset of transition. However, these data are only indicative, since tunnel-wall radiated noise affected the model boundary layer near the point of transition, and thus the tunnel noise may have led to an earlier onset of transition on the model.

Difficulties with Hot-Wire Measurements in Short-Duration Tunnels

When the Purdue Mach-6 tunnel first became quiet at high Reynolds numbers, Rufer was in the process of measuring second-mode waves on a 7-deg. half-angle sharp cone at zero angle of attack, using hot wires, the traditional technique [70, 71]. During the development of the Purdue Mach-6 tunnel as a Ludwieg tube, there were concerns about hot-wire survivability, but preliminary assessments suggested that the difficulties would not be large. However, the second-mode waves could only be measured under conventional noise conditions, since their amplitude was below the electronic noise floor under quiet conditions. Furthermore, difficulties with survival and calibration of the high-frequency hot wires yielded very limited quantitative data, despite considerable efforts. Because of the intrusive nature of the hot-wire probe, the data were also limited to a single point per run, although it *is* often very useful and sometimes critical to be able to put the sensor at a particular position above the wall and within the flowfield [39].

The long run times available at NASA Langley and at the Jet Propulson Lab [72] vastly reduced the difficulty in getting hot wires to survive startup and shutdown, but these long run times (measured in hours) are also very expensive and no longer readily affordable. The Langley Mach-6 quiet nozzle is now running again at Texas A&M University, with moderate run-times of 30-40 sec., which enable the hot wires to be parked in a protected location during startup and shutdown [73]. This longer runtime will enable traversing the hot wires from a parking position, measuring in a variety of locations, and then parking the hot wire again before shutdown. The A&M facility will therefore have much more capability for operating with hot wires, complementing the optical-access capabilities of the Purdue facility. However, these moderate run times require the use of ejectors to achieve low pressures downstream of the nozzle, and the inefficiency of ejectors again leads to increased operating costs. Even with the longer runtime, difficulties with the frequency response and productivity of hot wires has lead the Texas group towards other instrumentation [43]. Progress within the Texas A&M effort is to be reported in the following paper at the present conference [74].

Low-speed experiments with hot wires are often carried out over tens of hours consecutively, moving the hot wires with an automated traverse, and mapping the flowfields in great detail (e.g., Refs. [75, 76]). This has been a very productive approach at these speeds. With the larger budgets that were at one time available, a similar approach might be productive even at hypersonic speeds, where the energy requirements and associated costs are orders of magnitude higher. In the early 1960's, for example, the Univ. of Minnesota operated a continuous-flow tunnel with a 6x9-inch test section at Mach 5, using 4800HP, and supported by the Air Force Office of Scientific Research, probably only in part [77]. A somewhat smaller facility operated at Caltech for many years in the 1950's and 1960's, but was shut down when the funding decreased and it became too expensive to operate (e.g., Ref. [78]).

However, when the author began working on hypersonic transition in 1990, near the end of the Cold War, it seemed clear that budgets of this kind were no longer feasible. Measurements of hypersonic instability and transition would only be feasible if funding for them could be sustained over a long period of time, in order to develop the necessary high-frequency low-amplitude instrumentation. Probable budgets would require new facilities to be much more affordable, which meant relatively short runtimes [79]. High-speed experiments would generate high-frequency instabilities, and relatively short run times would be sufficient to measure these, if the instrumentation could be successfully developed. Circa 2005, it became evident that hot wires were not robust enough to achieve good productivity even in the Mach-6 quiet tunnel with its highly filtered air. More robust sensors were needed; furthermore, if they could be developed, they could also be used in other tunnels, enabling the study of the mechanisms of transition at a variety of Mach numbers and enthalpies.

Measurements with Fast Pressure Sensors

These difficulties with hot-wire survivability and productivity led to an increased effort to find alternative instrumentation. Fortunately, in Jan. 2005 Fujii et al. reported that second-mode waves could be measured with PCB-132 surface pressure sensors [80, 81]. If these sensors could be used successfully at Purdue and other sites, measurements of second-mode waves might become common, and comparisons between different tunnels could then be made. In Jan. 2005, Dr. Fujii was kind enough to communicate the exact type of sensors that were used, and a sample sensor was purchased by Purdue, arriving in Feb. 2005. However, this effort then sat on the back burner, with the Purdue researchers focused on getting the nozzle to run quiet at high Reynolds numbers. Progress occurred only due to a

cooperation with T.U. Braunschweig, who sent Estorf on a visit to Purdue in Jan. 2007, with his own cone and sensors. Estorf very quickly became productive with the tunnel and sensors, and reported very interesting results in Jan. 2008 [60].

Estorf measured using the same 7-deg. half-angle sharp cone, apparently with the same sensors, in the Mach-6 tunnels at both Purdue and Braunschweig. Fig. 5 shows measurements in the Purdue tunnel under quiet flow at Mach 6, compared to measurements under noisy flow in the same tunnel at Mach 5.8 (the noisy flow measurements are at a slightly lower Mach number due to the thicker nozzle-wall boundary layer). A second-mode instability wave is evident under both noisy and quiet flow, at a Reynolds number $Re_x \simeq 2.21 \times 10^6$, where x is the axial position of the sensor. The tunnel conditions are reported with the figure; the quiet tunnel run is at a slightly higher stagnation pressure, in order to match the Reynolds number at the slightly higher Mach number. The model temperature is near 300K, since the run-time is short.

The wave has almost the same frequency under both quiet and noisy flow, about 220 kHz. Estorf reports that the waves are about 450 times smaller under quiet flow. Thus, the same cone operated at almost the same mean-flow condition yields the same frequency of second-mode wave, presumably the one that is most amplified between the neutral curve and the measurement location. The waves are smaller under quiet flow because their initial amplitude is lower. If the receptivity is linear, the freestream content at 220kHz under quiet and noisy flow might be expected to differ by this factor of 450, but this would be very difficult to measure, particularly under quiet flow when the signals are exceedingly small, even at lower frequencies. Thus, it is very difficult to check a linear receptivity assumption here.

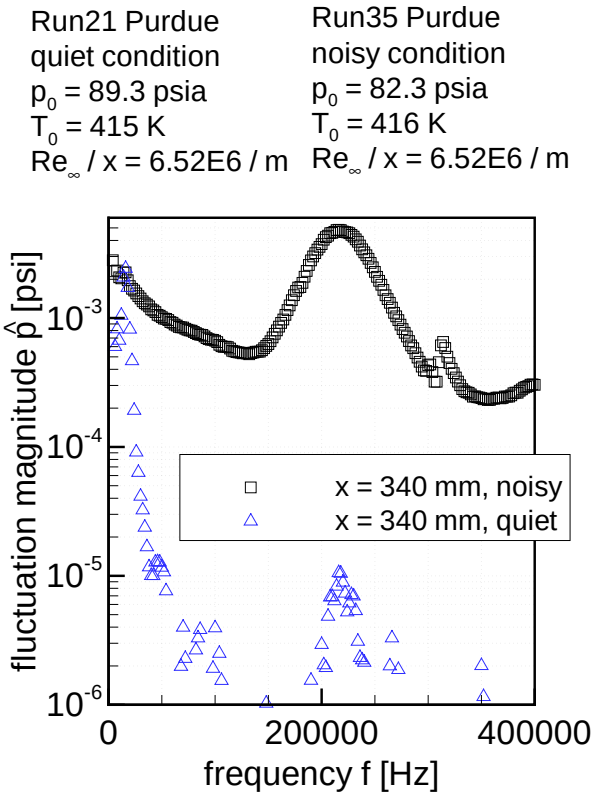

Figure 5: Spectra of pressure fluctuations measured in noisy and quiet flow at the same Reynolds numbers on the same cone with the same sensor. Replotted from Ref. [60, Fig. 8]

As Estorf notes, it would be good to check the amplification of the waves under quiet and noisy flow, to see if the amplification rates or amplitude ratios vary with the wave amplitudes. This is a classic method of checking linearity. However, this was not feasible under quiet flow, since the waves were too small to measure with any accuracy.

Estorf also measured the surface-pressure fluctuations on this same cone in the Braunschweig tunnel, along with the pitot-pressure fluctuations in the freestream. The composite plot is shown in Fig. 6. For the lower Reynolds number of $Re_x = 0.95 \times 10^6$, the most amplified second-mode wave at this particular sensor is at a frequency where the pitot-pressure

signal appears to be well above the noise. Thus, it would be possible to take the amplitude of this second-mode wave, infer the amplitude at the onset of instability, and infer an effective receptivity coefficient with respect to the freestream pitot fluctuations. This effective receptivity coefficient could then be compared to theoretical and computational models. At the higher Reynolds number, the most amplified frequency is higher, near the maximum that can be resolved in the pitot-pressure signal with acceptable signal-to-noise ratio, so this comparison is more difficult. It seems likely that further comparisons of this type would be fruitful, if reasonably accurate measurements of the signal amplitudes can be obtained.

Estorf also compared noisy-flow wave amplitudes in the Purdue and Braunschweig tunnels, as shown in Figs. 7 and 8. As the waves grow, saturate and break down to turbulence, the wave amplitude increases, reaches a maximum, and then decreases. This pattern has been seen many times in the last few years (see, for example, Ref. [61]). For the same cone operated at nearly the same Mach number, and very similar mean-flow conditions, *this nonlinear breakdown occurs at almost the same location in the two tunnels.* Since the details of the nonlinear breakdown process are expected to depend on the details of the freestream fluctuations [82], it is remarkable to see this level of agreement for two different tunnels that are expected to have significantly different noise levels. The figure suggests that the dependence of the nonlinear breakdown on freestream disturbances may not be all that sensitive. It also suggests that more comparisons of this kind are likely to be fruitful.

In Fig. 7, the spectral interval is 2000Hz, and in Fig. 8, the spectral interval is 5000Hz, but the amplitudes are corrected by $\sqrt{2.5}$ to match the amplitudes that would be seen with a spectral interval of 2000Hz. When the quiet-tunnel valve that controls the bleed-slot flow is closed, the flow spills over the bleed lip and trips the downstream boundary layer. Although one might think that this would yield a tunnel noise level that is higher than in a conventional tunnel without the bleed slot, it does not seem to, apparently because the noise radiated from the nozzle-wall boundary layer dominates. This was tested in the Purdue tunnel at high unit Reynolds numbers, where the nozzle-wall boundary layer is turbulent even with the bleeds open [69, 83]. However, the freestream fluctuations in the Purdue and Braunschweig tunnels will still be significantly different, even though the Mach numbers are almost the same, and the stagnation conditions are almost the same, since the Braunschweig nozzle is about 0.5m in diameter, and the Purdue nozzle is 0.24m in diameter. The change in the diameter and length of the nozzle will change the nozzle-wall turbulent boundary layer and thus the radiated noise in the freestream [52].

Effects of Tunnel Noise on the Nonlinear Breakdown

To obtain natural transition under fully quiet flow, where transition occurs well upstream of the onset of noise radiated from transition in the nozzle-wall boundary layer, it is necessary to build either a more-laminar quiet tunnel, or a more-unstable model. Since the Purdue nozzle became laminar past the exit to about 170 psia stagnation pressure, it provides about twice the quiet Reynolds number as the earlier NASA Langley nozzle. If the Langley work to flare a cone to enhance instability were also extended to a systematic stability-based design of the most-unstable axisymmetric model, natural transition under fully quiet flow might be achieved.

This approach was pursued back beginning in fall 2008, as described in Ref. [84] and a series of AIAA Paper sections [85, 83, 86, 87]. At first, transition was expected to occur near a computed N-factor near 10, as in the previous Langley data. Surprisingly, however, laminar flow was maintained to N factors near 17. Fig. 9 shows pressure-fluctuation spectra from the downstream sensor on the original flared cone, with a 1-mm nose radius, at stagnation temperatures near $160°C$, and four different stagnation pressures. For the first time, very large waves were successfully measured under fully quiet flow. As expected, the frequency of the amplified waves near 300kHz increases with stagnation pressure, as the boundary layer becomes thinner, and the amplitude of the waves increases. The largest waves become nonlinear, as evidenced by the appearance of a second harmonic near 600kHz.

The large amplitude of these waves becomes most evident when time traces are examined. Fig.10 shows a time-trace from the furthest-upstream sensor at the highest pressure shown in the previous plot. The signal is very clearly near-sinusoidal, with a peak-peak amplitude near 30% of the mean pressure. Since the waves had previously been barely detectable under quiet flow, it was really remarkable to obtain such simple measurements of really large waves.

The next set of measurements used a needle-like nose with a tip radius of 0.16 mm, in order to in-

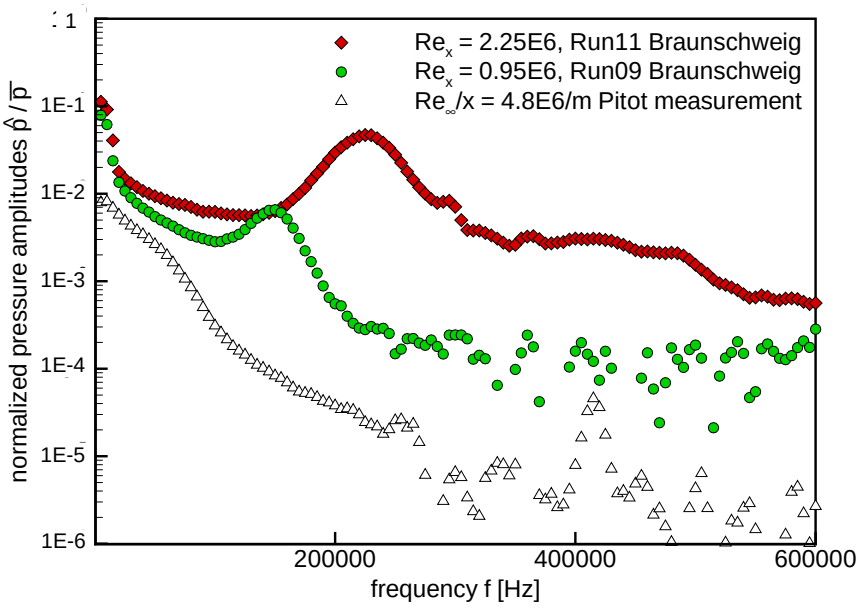

Figure 6: Surface pressure fluctuations normalized by calculated edge pressures at two different Reynolds numbers compared to normalized pitot pressure fluctuations measured in Braunschweig tunnel. From Ref. [60, Fig. 9]

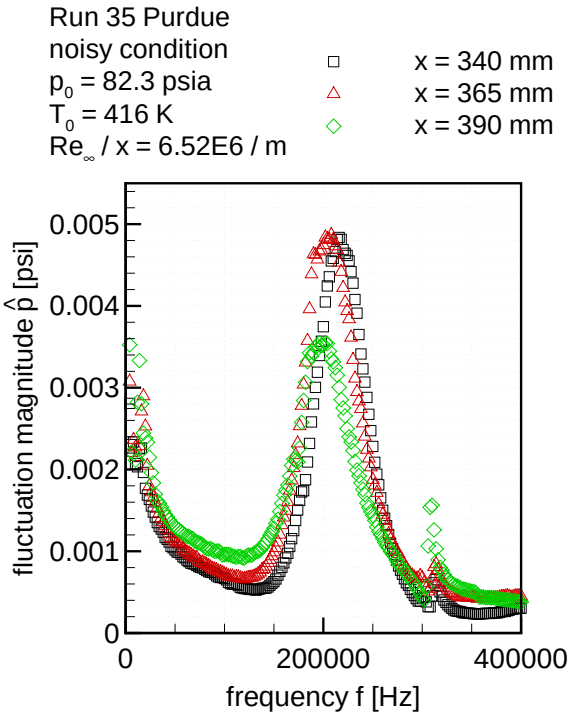

Figure 7: Spectra of pressure fluctuations measured in noisy Mach-5.8 flow at Purdue. Replotted from Ref. [60, Fig. 7a]

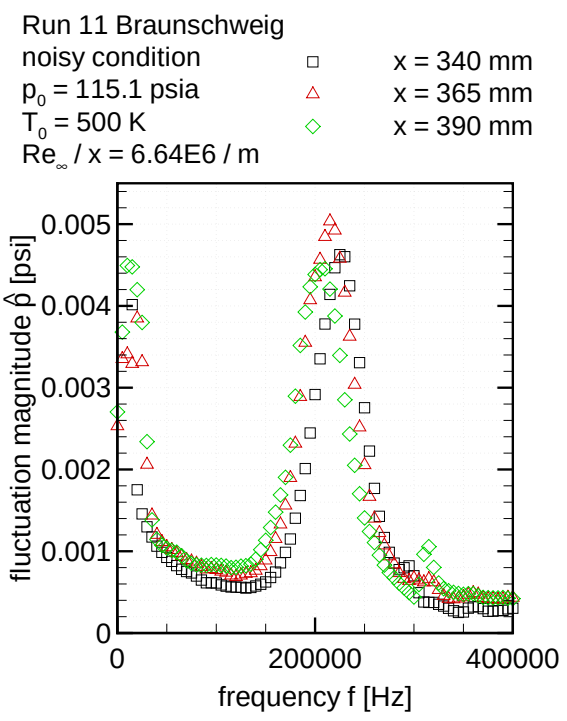

Figure 8: Spectra of pressure fluctuations measured in noisy Mach-5.8 flow at Braunschweig. Replotted from Ref. [60, Fig. 7b]

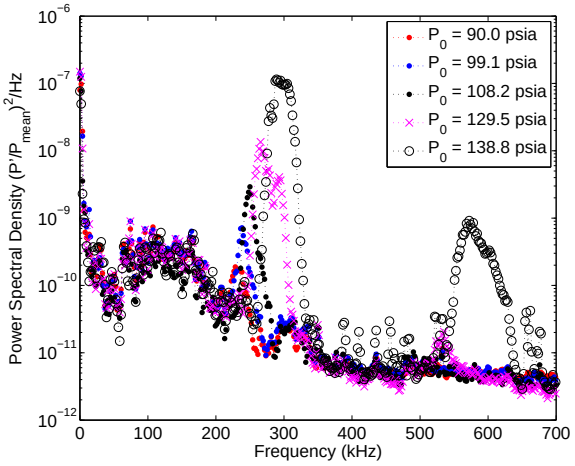

Figure 9: PCB measurements from quiet runs with sensor at $x = 0.4$m. From Ref. [85, Fig. 16]

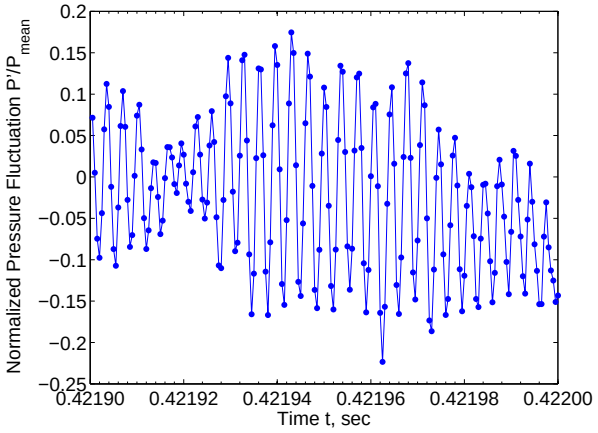

Figure 10: PCB time-trace showing large second-mode waves under quiet flow. $P_0 = 138.8$ psia with sensor at $x = 0.2$m. From Ref. [85, Fig. 17]

crease the amplitude of the waves. With sufficiently larger waves, transition might occur on the cone even under fully quiet flow. Although transition was *not* clearly observed, surprising streamwise streaks were evident in the temperature-sensitive paint images, as shown in Fig. 11. Even more surprisingly, the amplitude of the streaks increased, decreased, and then increased again. At the time, there was no known mechanism that could explain this phenomenon. However, at nearly the same time, a similar phenomena was observed in straight-cone computations by Laible and Fasel [59], thereby providing a possible mechanism. Görtler instabilities must of course also be considered on the flared cone, as discussed by Li et al. [88]. These streamwise streaks occurred only under quiet flow, which provided strong evidence that the nonlinear breakdown process for second-mode waves was strongly dependent on the background fluctuation environment. It may be that the earlier Langley experiments on the flared cones were affected by the higher levels of tunnel noise that were radiated onto the aft end of the models [89, 41].

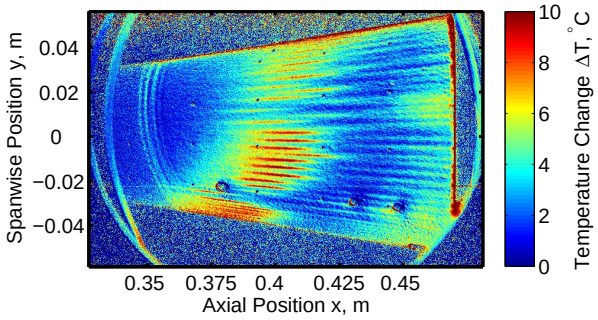

Figure 11: TSP image of qualitative heating on surface of flared cone at $P_0 = 140.3$ psia and $T_0 = 151.4°C$. From Ref. [83, Fig. 21a]

These effects of freestream noise on breakdown amplitude are likely to be of practical importance, as suggested by Fig. 12, which shows the computed N-factors for instability waves on the flared cone used for Fig. 10, at a slightly higher tunnel pressure. Surprisingly, there is no indication of transition near $N = 10$. Rather, transition is delayed to $N \simeq 17-20$, if in fact it really occurs on the cone before the end of the model. Perhaps the more highly

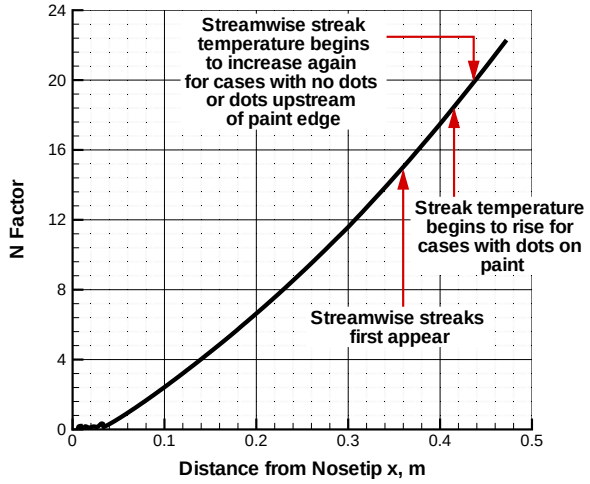

Figure 12: Computed N-factor for the flared cone at $P_o = 150$ psia and $T_o = 160°C$. Computations from Gronvall[86]. From Ref. [83, Fig. 26]

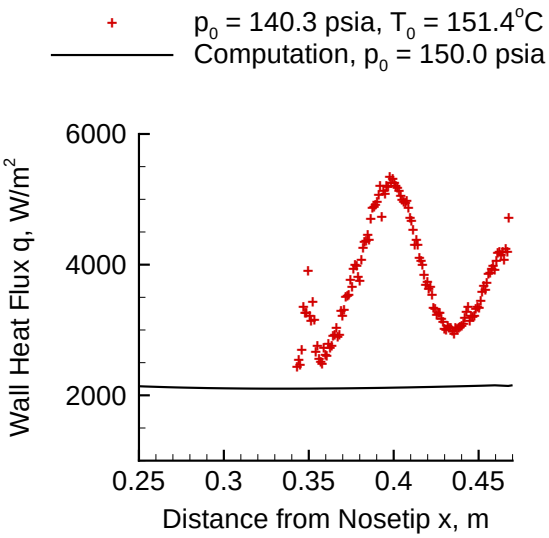

Figure 13: Streamwise heating and heat-transfer for the flared cone at $T_o = 160°C$. Adapted from Ref. [83, Fig. 25]

disturbed freestream that occurs under noisy flow causes larger 3D perturbations in the second-mode waves, leading to breakdown at smaller amplitudes.

The spanwise-average heat-transfer for a similar case is plotted vs. streamwise distance in Fig. 13. At $x \simeq 0.35$ m, the heat-transfer begins to rise above the computed laminar value, although the well-organized streamwise vortices suggest that the flow remains laminar, as in Borg's data on the X-51A forebody [90]. The heat-transfer rises by more than a factor of 2 as the vortices strength, but then falls by nearly a factor of 2 as the vortices weaken again. It seems that transition may occur near $x = 0.44$m, when the heat-transfer rises for the second time. This complex behavior was very surprising when first measured, but yields good qualitative agreement with the computations by Fasel's group for similar geometries [58, 91, 92]. However, quantitative comparisons remain to be obtained.

A series of experiments has been carried out to reduce the uncertainty in the location of the onset of transition for these flows. Although quiet flow can only be sustained to moderate Reynolds numbers, recent improvements in the quiet-flow Reynolds number enabled obtaining similar TSP images at slightly higher pressures. Fig. 14 shows the same pattern of streaks which appear and then weaken and then strengthen again. However, in this case, it appears that the flow may proceed all the way to full turbulence, at least towards the lower side of the nominally axisymmetric flow. The surface-pressure fluctuations near the aft end of the cone also suggest that the flow there is becoming fully turbulent [87, p. 17]. However, further experiments are clearly needed.

The nonlinear breakdown of the second-mode waves on these flared cones also yields evidence for the nonlinear saturation of the second-mode waves. To show this, Chou compiled data from Refs. [83, 87] and [84] to develop Fig. 15, which was not previously published. The computed N factors are shown using the solid line, referred to the right-hand axis, for this flow with T_0 near $160°C$. The PCB signal amplitudes are shown using the red circles, referred to the left-hand axis. The RMS second-mode wave amplitudes that are obtained from the power spectra show clear evidence of nonlinear saturation, which is somewhat similar to the saturation that occurs for stationary crossflow waves on swept wings [93]. However, the PCB surface-pressure signals are limited by spatial averaging and uncertainties in their calibrations [94], so further experiments are again needed.

Some further experiments were carried out by Luersen [95]. These focused on improving techniques for the application of small controlled roughness, in

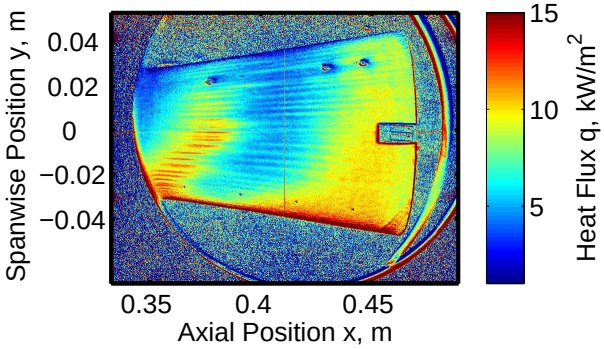

Figure 14: Heat flux on flared cone at $P_o = 163.7$ psia and $T_o = 151.5°C$ under quiet flow from left to right. From Ref. [87, Fig. 20]

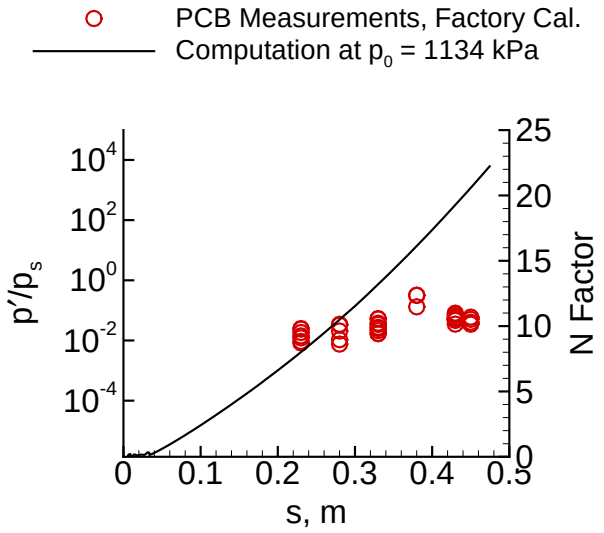

Figure 15: N-factor comparison for Purdue flared-cone experiment

order to induce the streamwise streaks under controlled condition. Luersen also performed successful experiments with a larger cone, achieving higher quiet Reynolds numbers. However, this work was only partially successful. The effort is now being carried on by Brandon Chynoweth.

The series of experiments on the flared cone shows fairly clearly that there is a dramatic effect of tunnel noise on the breakdown of large second-mode waves. It shows that this nonlinear breakdown is of practical significance, since the N factors at transition can be much larger than expected under quiet flow. It also shows that small upstream roughness can trigger the streamwise vortices that were an element of the breakdown process on these flared cones; thus, small upstream roughness can affect the transition location.

However, much remains to be resolved. The flare is needed to generate large second-mode waves under available quiet-flow conditions, but the flare also induces the Görtler instability, which may change the second-mode breakdown process. The degree to which the nonlinear breakdown can be controlled or influenced by small upstream roughness remains mostly unknown. Quantitative comparisons are needed between measurements and computations; such an effort seems likely to require several years of focused and coordinated work, which may be difficult to organize.

Mechanism-Based Methods for Crossflow-Induced Transition

A 7-deg. half-angle cone near 6-deg. angle of attack is being used by several researchers as another canonical configuration for experimental and computational study at Mach 6 (e.g., Refs. [96, 97, 98, 99, 100, 101]). Although much can be inferred from the extensive literature on swept wings at low speeds, it is not yet clear how much will be different. The bow shock that is present on realistic geometries converts freestream acoustic and vorticity perturbations into all other forms [32], so the low-speed information here must be adapted with care. Small surface roughness seems likely to trigger the stationary crossflow instability, as at low speeds, but although this phenomena has been observed at Mach 3.5, it is only beginning to be observed at hypersonics speeds in a clearcut way [102]. It is also not yet clear how tunnel noise will affect the receptivity, growth and nonlinear breakdown of these waves. The 7-deg. cone at 6-deg. AoA is a good generic geometry that is being studied by many researchers

in an effort to work out some of these issues. The 2:1 elliptic cross-section cone flown for HIFiRE-5 is also being studied by several researchers.

A substantial effort will be needed to review this developing body of literature. Here, there is space and time only to highlight some surprising recent results from Borg's measurements on the HIFiRE-5 geometry [103]. Fast pressure sensors were placed off the centerline of the model, near the aft end, in a region where traveling crossflow waves were predicted to reach $N \simeq 13$. [104] Based on low-speed experiments on swept wings, the traveling waves were expected to dominate under noisy conditions, with the stationary waves dominating under quiet conditions [6].

Surprisingly, a different effect has been observed in the Purdue quiet tunnel at Mach 6, as shown in Figs. 16 and 17. The measurements are again all at T_0 near $160°C$, on a model near room temperature, at various stagnation pressures, with the freestream unit Reynolds numbers listed in the legends. Fig. 16 was obtained under quiet flow. Traveling crossflow waves are evident near 40-50kHz, with amplitudes that increase with Reynolds number. The wave angle and phase speeds of these waves agree well with the computations, so these are clearly traveling crossflow waves, as shown in Ref. [103]. Surprisingly, Fig. 17 shows that under noisy flow, there is no evidence of traveling crossflow waves, even at very low Reynolds numbers.

The cause of this unexpected phenomena is not clear. It seems possible that transition occurs due to a different mechanism under noisy flow, leading to the broadband spectra observed in the right-hand part of the figure. However, this seems very unlikely at the lower Reynolds numbers. Further research is needed to understand this effect.

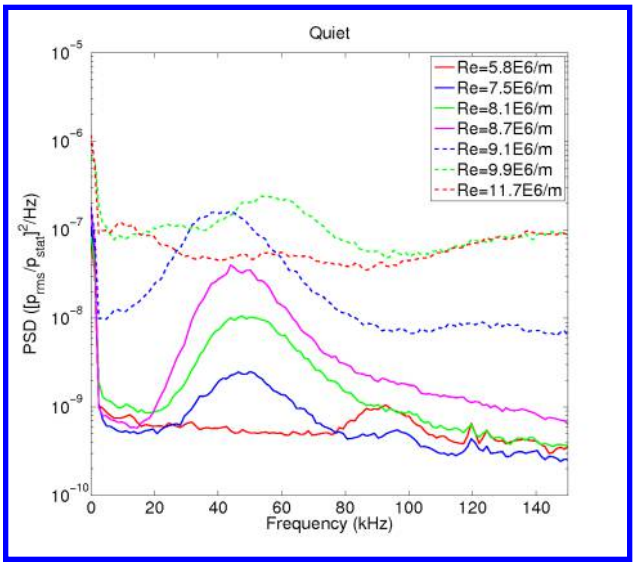

Figure 16: Traveling Crossflow Waves on the HiFire-5 Elliptic Cone Under Quiet Conditions. From Ref. [103]

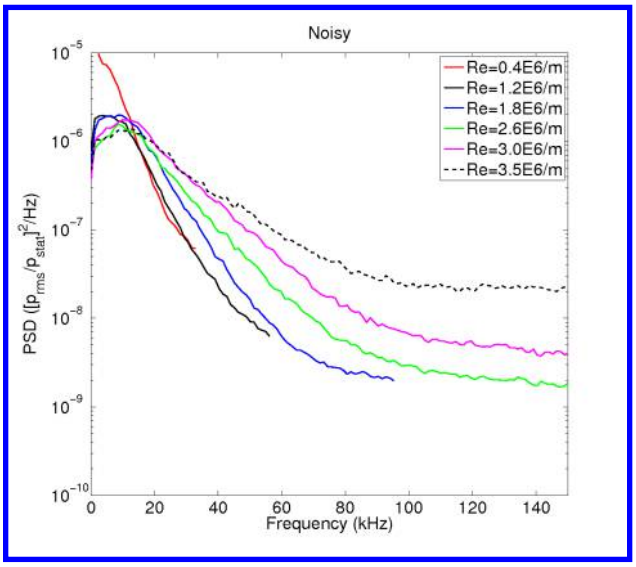

Figure 17: Traveling Crossflow Waves on the HiFire-5 Elliptic Cone Under Noisy Conditions. From Ref. [103]

Mechanism-Based Methods for Transition Induced by Isolated Roughness

Roughness can have many different effects on hypersonic transition, depending on the properties of the mean flow and the smooth-wall instabilities [14, 15]. One particular example is the possible generation of transition behind an isolated roughness due to the instabilities of the roughness-induced mean flow. Both computations and experiments are

being carried out in this area by several researchers, with promising results to date. Here again, time and space are sufficient only to cite a few of the recent papers [39, 105, 38, 106, 107].

Mechanism-Based Methods for First-Mode-Induced Transition

Even at hypersonic speeds, transition may be induced by the first-mode instability, if the edge Mach number is lowered by bluntness, angle of attack, or some other phenomena, or if the surface temperature is sufficiently high. For example, a possibly-dominant first-mode instability was computed in 2009 for the Mars Science Laboratory vehicle [108]. However, modern computations of this kind have not yet been verified with instability-wave measurements, due in part to the fragile nature of the hot-wire instrumentation that was once the only method available. It seems probable that the same kinds of fast surface pressure sensors that are now used to measure second-mode waves might also be used to measure these first-mode waves. However, this idea remains to be confirmed [102].

Methods for Predicting Transition Induced by Other Mechanisms

Although the first-mode, second-mode and crossflow instabilities are fairly well known, technological surprise remains a substantial risk for future vehicle designs, if a number of other phenomena are not better understood. A small-bluntness circular cone at angle of attack is representative of gliding hypersonic vehicles, yet there is presently no theory that can explain some of the critical phenomena observed in previous ground tests. For a hypersonic slender cone at zero angle of attack, transition first moves aft as the nose bluntness is increased from near-sharp radii. This is because the entropy layer generated by the bluntness stabilizes the cone boundary layer, as is reasonably well understood. However, for further increases in nose radius, transition reverses, and begins to move forwards again [109]. The mechanism for this reversal is not known, although it seems that the reversal mechanism suddenly makes frustum transition sensitive to nosetip roughness.

There is a second surprising phenomena which may be closely related. When cones with small bluntness are placed at angle of attack, transition often occurs first on the leeward ray. The low-momentum fluid within the boundary layer is swept around to the lee ray by the crossflow pressure gradient, generating a thick and highly unstable lee-ray boundary layer. Thus, transition is usually initiated by the crossflow instability on the yaw sides of the cone, or by a streamwise instability on the lee ray. This much is reasonably well understood. However, when the nose radius or Reynolds number is increased further, transition then occurs first on the windward ray [109]. The mechanism for this is again unknown, although several concepts have been proposed.

Lacking any clear understanding of these mechanisms, it is not yet possible to scale these phenomena, or to determine when they might occur, so they create a substantial risk of expensive surprises in future development programs. These kinds of technological surprises will remain a risk for new hypersonic programs, yet such risks must be accepted and addressed in order to remain a world leader in aerospace.

Summary

Transition is famously sensitive to apparently small factors like tunnel noise, surface roughness, and so on. There may be new hypersonic transition mechanisms that remain to be identified. Hypervelocity instability and transition is not yet well understood, so an effective research and development effort should combine theory, numerical simulation, ground and flight experiments to efficiently retire these risks, reduce uncertainties, and improve designs. Since no single ground-test facility can simulate all aspects of hypersonic flight, it appears necessary to make measurements of instability and transition in a variety of facilities, comparing the results from each to various numerical simulations, in order to determine the critical instability mechanisms and to develop and validate the computations. This will require measuring the flow quality in the various facilities so that the effect of necessarily limited flow quality can be determined. In cold tunnels, the freestream fluctuations form the dominant flow-quality issue, although high-enthalpy tunnels may also need to investigate their chemical composition. The past half-century has shown that it is not possible to sort out the various parametric effects using only measurements of transition itself. Rather, the experiments must measure the instability mechanisms and the freestream fluctuations as well as the transition location. One element in such a program must remain the development and use of quiet hypersonic wind tunnels, with low noise levels that are comparable to flight.

Acknowledgements

The author's research would not have been possible without the long-term stable funding that has been provided by AFOSR. Funding has also been provided by Sandia National Laboratories and by NASA. Many people have provided help over many years, including Eli Reshotko of Case Western Reserve University, Ken Stetson of AFRL, Ivan Beckwith et al. from NASA Langley, Jim Kendall of JPL, and many others, too numerous to mention.

REFERENCES

[1] D. M. Bushnell. Notes on initial disturbance fields for the transition problem. In M. Y. Hussaini and R.G. Voigt, editors, *Instability and Transition, Volume I*, pages 217–232, Berlin, 1990. Springer-Verlag. Materials of the workshop held May 15 – June 9,1989 in Hampton, Virginia.

[2] William S. Saric, Helen L. Reed, and Edward J. Kerschen. Boundary-layer receptivity to freestream disturbances. *Annual Reviews of Fluid Mechanics*, 34:291–319, 2002.

[3] L. M. Mack. Boundary layer linear stability theory. In *Report 709, Special Course on Stability and Transition of Laminar Flow*, pages 1–81. AGARD, March 1984.

[4] Alexander Fedorov. Transition and stability of high-speed boundary layers. *Annual Reviews of Fluid Mechanics*, 43:79–95, 2011.

[5] D. Arnal and G. Casalis. Laminar-turbulent transition prediction in three-dimensional flows. *Progress in Aerospace Sciences*, 36(2):173–191, February 2000.

[6] H. Bippes. Basic experiments on transition in three-dimensional boundary layers dominated by crossflow instability. *Progress in Aerospace Sciences*, 35:363–412, 1999.

[7] W.S. Saric, H.L. Reed, and E.B. White. Stability and transition of three-dimensional boundary layers. *Annual Review of Fluid Mechanics*, 35:413–440, 2003.

[8] J.M. Floryan. On the Görtler instability of boundary layers. *Progress in Aerospace Sciences*, 28:235–271, 1991.

[9] William S. Saric. Görtler vortices. *Annual Review of Fluid Mechanics*, 26:379–409, 1994.

[10] K. Fujii and H. G. Hornung. Experimental investigation of high-enthalpy effects on attachment line boundary layer transition. *AIAA J.*, 41(7), July 2003.

[11] H.G. Hornung and P. Lemieux. Shock layer instability near the Newtonian limit of hypervelocity flows. *Physics of Fluids*, 13(8):2394–2402, August 2001.

[12] Scott Berry and Thomas Horvath. Discrete roughness transition for hypersonic flight vehicles. *J. of Spacecraft and Rockets*, 45(2):216–227, March-April 2008.

[13] Daniel C. Reda. Review and synthesis of roughness-dominated transition correlations for reentry applications. *J. of Spacecraft and Rockets*, 39(2):161–167, March-April 2002.

[14] Steven P. Schneider. Effects of roughness on hypersonic boundary-layer transition. *Journal of Spacecraft and Rockets*, 45(2):193–209, Mar.-Apr. 2008.

[15] Steven P. Schneider. Hypersonic boundary-layer transition on blunt bodies with roughness. *Journal of Spacecraft and Rockets*, 45(6):1090–1105, Nov.-Dec. 2008.

[16] Steven P. Schneider. Hypersonic boundary-layer transition with ablation and blowing. *Journal of Spacecraft and Rockets*, 47(2):225–237, Mar.-Apr. 2010.

[17] Eli Reshotko. Transition issues for atmospheric entry. *Journal of Spacecraft and Rockets*, 45(2):161–164, March-April 2008.

[18] Th. Herbert. Secondary instability of boundary layers. *Annual Reviews of Fluid Mechanics*, 20:487–526, 1988.

[19] R. Narasimha. The laminar-turbulent transition zone in the turbulent boundary layer. *Progress in Aerospace Sciences*, 22:29–80, 1985.

[20] A.M. Berkowitz, C.L. Kyriss, and A. Martellucci. Boundary layer transition flight test observations. Paper 77-125, AIAA, January 1977.

[21] K. Stetson and R. Kimmel. On hypersonic boundary-layer stability. Paper 92-0737, AIAA, January 1992.

[22] J. D. Crouch. Modeling transition physics for laminar flow control. Paper 2008-3832, AIAA, June 2008.

[23] Helen L. Reed, William S. Saric, and Daniel Arnal. Linear stability theory applied to boundary layers. *Annual Reviews of Fluid Mechanics*, 28:389–428, 1996.

[24] Heath B. Johnson and Graham V. Candler. Analysis of laminar-turbulent transition in hypersonic flight using PSE-Chem. Paper 2006-3057, AIAA, June 2006.

[25] Mujeeb R. Malik. Hypersonic flight transition data analysis using parabolized stability equations with chemistry effects. *Journal of Spacecraft and Rockets*, 40(3):332–344, May-June 2003.

[26] Geza Schrauf. Large-scale laminar-flow tests evaluated with linear stability theory. *AIAA Journal of Aircraft*, 41(2):224–230, March-April 2004.

[27] Christopher A.C. Ward, Bradley M. Wheaton, Amanda Chou, Dennis C. Berridge, Laura E. Letterman, Ryan P.K. Luersen, and Steven P. Schneider. Hypersonic boundary-layer transition experiments in the Boeing/AFOSR Mach-6 quiet tunnel. Paper 2012-0282, AIAA, January 2012.

[28] L. Kleiser and T. Zang. Numerical simulation of transition in wall-bounded shear flows. *Annual Reviews of Fluid Mechanics*, 23:495–537, 1991.

[29] X. Zhong and X. Wang. Direct numerical simulation on the receptivity, instability and transition of hypersonic boundary layers. *Annual Reviews of Fluid Mechanics*, 44:527–561, 2012.

[30] Fei Li, Meelan Choudhari, C.-L. Chang, J. White, R. Kimmel, D. Adamczak, M. Borg, S. Stanfield, and M. Smith. Stability analysis for HIFiRE experiments. Paper 2012-2961, AIAA, June 2012.

[31] Th. Herbert. Parabolized stability equations. *Ann. Rev. Fluid Mech.*, 29:245–284, 1997.

[32] Steven P. Schneider. Effects of high-speed tunnel noise on laminar-turbulent transition. *Journal of Spacecraft and Rockets*, 38(3):323–333, May–June 2001.

[33] Leslie S.G. Kovasznay. Turbulence in supersonic flow. *J. of the Aeronautical Sciences*, 20:657–682, October 1953.

[34] Lian Duan and Meelan Choudhari. Numerical study of pressure fluctuations due to a Mach-6 turbulent boundary layer. Paper 2013-0532, AIAA, January 2013.

[35] Chau-Lyan Chang. LASTRAC.3d: Transition prediction in 3D boundary layers. Paper 2004-2542, AIAA, June 2004.

[36] Thorwald Herbert. On the stability of 3D boundary layers. Paper 97-1961, AIAA, June 1997.

[37] Graham V. Candler. Nonequilibrium processes in hypervelocity flows: an analysis of carbon ablation models. Paper 2012-0724, AIAA, January 2012.

[38] Bradley M. Wheaton, Steven P. Schneider, Matthew D. Bartkowicz, P. K. Subbareddy, and Graham V. Candler. Numerical and experimental comparison of roughness-induced instabilities at Mach 6. Paper 2011-3248, AIAA, June 2011.

[39] Bradley M. Wheaton and Steven P. Schneider. Roughness-induced instability in a hypersonic boundary layer. *AIAA Journal*, 50(6):1245–1256, 2012.

[40] I.E. Beckwith and C.G. Miller III. Aerothermodynamics and transition in high-speed wind tunnels at NASA Langley. *Annual Review of Fluid Mechanics*, 22:419–439, 1990.

[41] Steven P. Schneider. Development of hypersonic quiet tunnels. *Journal of Spacecraft and Rockets*, 45(4):641–664, Jul.-Aug. 2008.

[42] Katya M. Casper, Heath B. Johnson, and Steven P. Schneider. Effect of freestream noise on roughness-induced transition for a slender cone. *J. Spacecraft and Rockets*, 48(3):406–413, May-June 2011.

[43] Jerrod W. Hofferth, Raymond A. Humble, Daniel C. Floryan, and William S. Saric. High-bandwidth optical measurements of the second-mode instability in a Mach 6 quiet tunnel. Paper 2013-0378, AIAA, January 2013.

[44] Chuan-Hong Zhang, Qing Tang, and Cun-Biao Lee. Hypersonic boundary-layer transition on a flared cone. *Acta Mechanica Sinica*, 29(1):48–53, 2013. In English.

[45] John J. Bertin and Russell M. Cummings. Fifty years of hypersonics: where we've been, where we're going. *Progress in Aerospace Sciences*, 39:511–536, 2003.

[46] Heath B. Johnson, Graham V. Candler, and Christopher R. Alba. Three-dimensional hypersonic boundary layer stability analysis with STABL-3D. Paper 2010-5005, AIAA, June 2010.

[47] H. Tanno, T. Komuro, K. Sato, K. Itoh, and M. Takahasi. Measurements of surface pressure fluctuation in hypersonic high-enthalpy boundary layer on a 7-degree cone model. Paper 2011-3889, AIAA, June 2011.

[48] T. Wadhams, M. MacLean, and M. Holden. Recent experimental studies of high-speed boundary-layer transition in LENS facilities to further the development of predictive tools for boundary layer transition in flight. Paper 2012-0470, AIAA, January 2012.

[49] N.J. Parziale, J.E. Shepherd, and H. G. Hornung. Differential interferometric measurement of instability in a hypersonic boundary-layer. *AIAA Journal*, 51(3):750–753, March 2013.

[50] Matthew P. Borg, Roger L. Kimmel, and Scott Stanfield. Crossflow instability for HIFiRE-5 in a quiet hypersonic wind tunnel. Paper 2012-2821, AIAA, June 2012. See also paper from NATO-RTO-MP-AVT-200, April 2012.

[51] Steven P. Schneider. Summary of hypersonic transition research coordinated through NATO RTO AVT-136. Paper 2010-1466, AIAA, January 2010.

[52] Samuel R. Pate. Effects of wind tunnel disturbances on boundary-layer transition with emphasis on radiated noise: A review. Paper 80-0431, AIAA, March 1980. Paper was distributed in person at the conference, and missed the usual archiving. Available online from DTIC as citation AD-A384962.

[53] Steven P. Schneider. Final report for AFOSR grant FA9550-08-1-0290 – Hypersonic laminar-turbulent transition on slender cones at zero angle of attack: Measurements in support of mechanism-based models for scaling ground-test data to flight. Final Report AFRL-OSR-VA-TR-2012-0261, AFOSR, April 2011. DTIC citation AD-A563803. 17 pages.

[54] A.V. Fedorov, A. Ryzhov, and V. Soudakov. Numerical and theoretical modeling of supersonic boundary-layer receptivity to temperature spottiness. Paper 2011-3077, AIAA, June 2011.

[55] Alex Bounitch, Daniel R. Lewis, and John F. Lafferty. Improved measurements of 'tunnel noise' pressure fluctuations in the AEDC hypervelocity wind tunnel no. 9. Paper 2011-1200, AIAA, January 2011.

[56] A.V. Fedorov and M.V. Koslov. Receptivity of high-speed boundary layer to solid particulates. Paper 2011-3925, AIAA, June 2011.

[57] A.V. Fedorov. Theoretical modeling of TS-dominated transition induced by solid particulates. Paper 2013-0668, AIAA, January 2013.

[58] J. Sivasubrahmanian and H. Fasel. Numerical investigation of laminar-turbulent transition in a cone boundary layer at Mach 6. Paper 2011-3562, AIAA, June 2011.

[59] A.C. Laible and H. Fasel. Numerical investigation of hypersonic transition for a flared and a straight cone at Mach 6. Paper 2011-3565, AIAA, June 2011.

[60] Malte Estorf, Rolf Radespiel, Steven P. Schneider, Heath B. Johnson, and Stefan Hein. Surface-pressure measurements of second-mode instability in quiet hypersonic flow. Paper 2008-1153, AIAA, January 2008.

[61] Dennis C. Berridge, Katya M. Casper, Shann J. Rufer, Christopher R. Alba, Daniel R. Lewis, Steven J. Beresh, and Steven P. Schneider. Measurements and computations of second-mode instability waves in three hypersonic wind tunnels. Paper 2010-5002, AIAA, June 2010.

[62] Katya M. Casper. Hypersonic wind-tunnel measurements of boundary-layer pressure fluctuations. Master's thesis, School of Aeronautics and Astronautics, Purdue University, August 2009.

[63] Ian J. Lyttle, Helen L. Reed, Alexander N. Shiplyuk, Anatoly A. Maslov, Dmitry A. Buntin, Eugene V. Burov, and Steven P. Schneider. Numerical-experimental comparisons of second-mode behavior for blunted cones. *AIAA Journal*, 43(8):1734–1743, August 2005.

[64] Steven P. Schneider. Hypersonic laminar instability on round cones near zero angle of attack. Paper 2001-0206, AIAA, January 2001.

[65] J. Donaldson and S. Coulter. A review of freestream flow fluctuation and steady-state flow quality measurements in the AEDC/VKF supersonic tunnel A and hypersonic tunnel B. Paper 95-6137, AIAA, April 1995.

[66] W.T. Strike, Jr., J.C. Donaldson, and D.K. Beale. Test section turbulence in the AEDC/VKF supersonic/hypersonic wind tunnels. Technical Report AEDC-TR-81-5, AEDC, July 1981.

[67] A.A. Maslov. Experimental study of stability and transition of hypersonic boundary layer around blunted cone. Technical report, Institute of Theoretical and Applied Mechanics, Russian Academy of Sciences, Siberian Branch, Novosibirsk, Russia, December 2001. Final Technical Report, International Science and Technology Center Grant 1863-2000. Funded by the European Office of Aerospace Research and Development, U.S.A.F. Defense Technical Information Center citation AD-A408241.

[68] Stephen P. Wilkinson. A review of hypersonic boundary layer stability experiments in a quiet Mach 6 wind tunnel. Paper 97-1819, AIAA, June 1997.

[69] Laura-cheri E. Steen. Characterization and development of nozzles for a hypersonic quiet wind tunnel. Master's thesis, School of Aeronautics and Astronautics, Purdue University, December 2010.

[70] Shann J. Rufer. *Hot-Wire Measurements of Instability Waves on Sharp and Blunt Cones at Mach 6*. PhD thesis, School of Aeronautics and Astronautics, Purdue University, December 2005.

[71] Shann J. Rufer and Steven P. Schneider. Hot-wire measurements of instability waves on cones at Mach 6. Paper 2006-3054, AIAA, June 2006.

[72] J. Kendall. Wind tunnel experiments relating to supersonic and hypersonic boundary-layer transition. *AIAA Journal*, 13:290–299, March 1975.

[73] Jerrod W. Hofferth and William S. Saric. Boundary-layer transition on a flared cone in the Texas A&M Mach 6 quiet tunnel. Paper 2012-0923, AIAA, January 2012.

[74] W. S. Saric, H.L. Reed, and R.D. Bowersox. Hypersonic boundary-layer laminar-turbulent transition. Paper 2013-XXXX, AIAA, June 2013.

[75] F. Gökhan Ergin and Edward B. White. Unsteady and transitional flows behind roughness elements. *AIAA Journal*, 44(11):2504–2514, November 2006.

[76] R.H. Radeztsky, M.S. Reibert, and W.S. Saric. Effect of isolated micron-sized roughness on transition in swept-wing flows. *AIAA J.*, 37(11):1370–1377, November 1999.

[77] C.J. Scott. Experimental investigation of laminar heat transfer and transition with foreign gas injection on a 16-deg. porous cone at Mach 5. Technical Report AFOSR-TN-60-1370, University of Minnesota, October 1960. DTIC citation AD258009. Rosemount Aeronautical Laboratories Research Report No. 174.

[78] John E. Lewis. *Experimental investigation of supersonic laminar, two-dimensional boundary layer separation in a compression corner with and without cooling*. PhD thesis, California Institute of Technology, 1967. Available from University Microfilms as dissertation number 67-8457.

[79] S.P. Schneider. A quiet-flow Ludwieg tube for experimental study of high speed boundary layer transition. Paper 91-5026, AIAA, December 1991.

[80] Keisuke Fujii. Experiment of two dimensional roughness effect on hypersonic boundary layer transition. *Journal of Spacecraft and Rockets*, 43(4):731–738, July-August 2006.

[81] Keisuke Fujii. An experiment of two dimensional roughness effect on hypersonic boundary layer transition. Paper 2005-0891, AIAA, January 2005.

[82] Yury S. Kachanov. Physical mechanisms of laminar-boundary-layer transition. *Annual Reviews of Fluid Mechanics*, 26:411–482, 1994.

[83] Christopher A.C. Ward, Bradley M. Wheaton, Amanda Chou, Peter L. Gilbert, Laura E.

Steen, and Steven P. Schneider. Boundary-layer transition measurements in a Mach-6 quiet tunnel. Paper 2010-4721, AIAA, June 2010.

[84] Amanda Chou. Characterization of laser-generated perturbations and instability measurements on a flared cone. Master's thesis, School of Aeronautics and Astronautics, Purdue University, December 2010.

[85] Brad M. Wheaton, Thomas J. Juliano, Dennis C. Berridge, Amanda Chou, Peter L. Gilbert, Katya M. Casper, Laura E. Steen, and Steven P. Schneider. Instability and transition measurements in the Mach-6 quiet tunnel. Paper 2009-3559, AIAA, June 2009.

[86] Dennis Berridge, Amanda Chou, Christopher Ward, Laura Steen, Peter Gilbert, Thomas Juliano, Steven Schneider, and Joel Gronvall. Hypersonic boundary-layer transition experiments in a Mach-6 quiet tunnel. Paper 2010-1061, AIAA, January 2010.

[87] Amanda Chou, Christopher A.C. Ward, Laura E. Letterman, Ryan P.K. Luersen, Matthew P. Borg, and Steven P. Schneider. Transition research with temperature-sensitive paints in the Boeing/AFOSR Mach-6 quiet tunnel. Paper 2011-3872, AIAA, June 2011.

[88] Fei Li, Meelan Choudhari, Chau-Lyan Chang, and Jeffrey White. Analysis of instabilities for non-axisymmetric hypersonic boundary layers over cones. Paper 2010-4643, AIAA, June 2010.

[89] S. Wilkinson. A review of hypersonic boundary layer stability experiments in a quiet Mach 6 wind tunnel. Paper 97-1819, AIAA, June 1997.

[90] Matthew P. Borg and Steven P. Schneider. Effect of freestream noise on roughness-induced transition for the X-51A forebody. *J. Spacecraft and Rockets*, 45(6):1106–1116, Nov.-Dec. 2008.

[91] J. Sivasubrahmanian and H. Fasel. Nonlinear stages of transition and breakdown in a boundary layer on a sharp cone at Mach 6. Paper 2012-0087, AIAA, January 2012.

[92] J. Sivasubrahmanian and H. Fasel. Direct numerical simulation of controlled transition in a boundary layer on a sharp cone at Mach 6. Paper 2013-0263, AIAA, January 2013.

[93] Mujeeb R. Malik, Fei Li, Meelan M. Choudhari, and Chau lyan Chang. Secondary instability of crossflow vortices and swept-wing boundary-layer transition. *Journal of Fluid Mechanics*, 399:85–115, 1999.

[94] Dennis C. Berridge. Measurements of second-mode instability waves in hypersonic boundary layers with a high-frequency pressure transducer. Master's thesis, School of Aeronautics and Astronautics, Purdue University, December 2010.

[95] Ryan P.K. Luersen. Techniques for application of roughness for manipulation of second-mode waves on a flared cone at Mach-6. Master's thesis, School of Aeronautics and Astronautics, Purdue University, December 2012.

[96] Aline van den Kroonenberg, Rolf Radespiel, Graham Candler, and Malte Estorf. Infrared measurements of boundary-layer transition on an inclined cone at Mach 6. Paper 2010-1063, AIAA, January 2010.

[97] Federico Munoz, Dirk Heitmann, and Rolf Radespiel. Instability modes in boundary layers of an inclined cone at Mach 6. Paper 2012-2823, AIAA, June 2012.

[98] Joseph J. Kuehl, Eduardo Perez, and Helen L. Reed. JoKHeR: NPSE simulations of hypersonic crossflow instability. Paper 2012-0921, AIAA, January 2012.

[99] Joel Gronvall, Heath Johnson, and Graham Candler. Hypersonic three-dimensional boundary-layer transition on a cone at angle of attack. Paper 2011-3561, AIAA, June 2011.

[100] Chan Y. Schuele, Thomas C. Corke, and Eric Matlis. Control of stationary cross-flow modes in a Mach 3.5 boundary layer using patterned passive and active roughness. *Journal of Fluid Mechanics*, 718:5–38, 2013.

[101] Lewis R. Owens, Michael A. Kegerise, and Stephen P. Wilkinson. Off-body boundary-layer measurement techniques development for supersonic low-disturbance flows. Paper 2011-0284, AIAA, January 2011.

[102] Christopher A.C. Ward, Roger R. Greenwood, Andrew D. Abney, and Steven P. Schneider.

Boundary-layer transition experiments in a hypersonic quiet tunnel. Paper 2013-XXXX, AIAA, June 2013. To appear in the June AIAA Fluid Dynamics Conference.

[103] Matthew P. Borg, Roger L. Kimmel, and Scott Stanfield. Traveling crossflow instability for HIFiRE-5 in a quiet hypersonic wind tunnel. Paper 2013-XXXX, AIAA, June 2013. To appear at the AIAA June 2013 meeting.

[104] M. Choudhari, C.-L. Chang, T. Jentink, F. Li, K. Berger, G. Candler, and R. Kimmel. Transition analysis for the HIFiRE-5 vehicle. Paper 2009-4056, AIAA, June 2009.

[105] Bradley M. Wheaton and Steven P. Schneider. Instability and transition due to near-critical roughness in a hypersonic laminar boundary layer. *J. of Spacecraft and Rockets*, 2013. To appear.

[106] Michael A. Kegerise, Lewis R. Owens, and Rudolph A. King. High-speed boundary-layer transition induced by an isolated roughness element. Paper 2010-4999, AIAA, June 2010.

[107] Meelan Choudhari, Fei Li, Minwei Wu, Chau-Lyan Chang, Jack Edwards, and Michael A. Kegerise Rudolph A. King. Laminar-turbulent transition behind discrete roughness elements in a high-speed boundary layer. Paper 2010-1575, AIAA, January 2010.

[108] C.-L. Chang, M.M. Choudhari, B.R. Hollis, and F. Li. Transition analysis for the Mars Science Laboratory entry vehicle. Paper 2009-4076, AIAA, June 2009.

[109] Steven P. Schneider. Hypersonic laminar-turbulent transition on circular cones and scramjet forebodies. *Progress in Aerospace Sciences*, 40(1-2):1–50, 2004.